Electronic Supplementary Material (ESI) for Environmental Science: Nano.

Insights into efficient bacterial inactivation over nano Ag/graphdiyne: dual activation of molecular oxygen and water molecules

Pan Chuanqi,[a‡] Zhang Biluan,[a‡] Pan Tingyu,[a‡] Huang Hui,[a‡] Song Siyi,[a] Cai Xitong,[a] Wang Yuhang,[a] Sun Hongwei,[a] Luo Zhu,[a] Zhang Lizhi[b] and Guo Yanbing [a, c, d]*

[a]Key Laboratory of Pesticide & Chemical Biology of Ministry of Education, Institute of Environmental and Applied Chemistry, College of Chemistry, Central China Normal University, Wuhan 430079, P. R. China
[b]School of Environmental Science and Engineering, Shanghai Jiao Tong University, Shanghai 200240, P. R. China
[c]Engineering Research Center of Photoenergy Utilization for Pollution Control and Carbon Reduction, Ministry of Education, College of Chemistry, Central China Normal University, Wuhan 430079, P. R. China
[d]Wuhan Institute of Photochemistry and Technology, Wuhan, 430082, China

Corresponding author: Yanbing Guo *E-mail: guoyanbing@mail.ccnu.edu.cn

Computational details

All calculations performed in this work were carried out by using density functional theory (DFT) as performed by Vienna ab initio simulation package (VASP).[1] Exchange-correlation functions are taken as the generalized gradient approximation (GGA) in the form of Perdew-Burke-Ernzerhof (PBE).[2] The projector augmented wave (PAW) method was used to replace the pseudopotential of inner core electrons and nucleus with the valence electrons.[3] The Kohn-Sham electron wave functions were expanded using the plane-wave functions with an energy cutoff of 400 eV. The optimization was considered convergence and each atom would be fully relaxed until the spring force between adjacent images was less than 0.05 eV $Å^{-1}$, the total energy change upon two steps for the electronic self-consistent field iteration was less than 1E-4 eV.

Single-layer graphdiyne (GDY) was simulated by a repeated slab model with a 2×2 supercell. The replicas of GDY layers were separated by a vacuum layer of 15 Å along the z-direction, which led to negligible interactions between the research system and their mirror images. Meanwhile, Ag_{38} cluster with the unique square Ag_4 lattice (squ-Ag_4) with a diameter of 1nm was adopted in this work. The 3×3×1 k-point meshes in Brillouin zone was sampled for structure optimization according to the Monk Horst−Pack scheme.[4] While for electronic property, the k-point sampling was 2×2×1.

Thermal stability of the catalysts was evaluated by molecular dynamics (MD) simulations, which adopt NVT ensemble, select Nose-Hoover hot bath, and the time step is 2 fs. We also investigated charge transfers of the Ag_{38}/ GDY by using the Bader charge analysis method. In addition, the Climbing images nudged elastic band (CL-NEB)[4]and dimer method [5] were used to carry out the transition state (TS). The number of inserting image was chosen by the formula “dist/0.8” derived from the difference-comparing scripts called dist.pl embedded in the transition state tools (VTST) software package compiled in VASP.

In order to describe the strength between transition metal and adsorbate in the adsorption process, we use the calculation method of d-band center theory as

$$\varepsilon d = \frac{\int_{-\infty}^{\infty} nd(\varepsilon)\varepsilon d\varepsilon}{\int_{-\infty}^{\infty} nd(\varepsilon)d\varepsilon}$$

The adsorption energy is highly linear with the the d band center,[6] thus the more positive the center of the d band is (moved close to the Fermi energy), the stronger the adsorption interaction is.

As for the adsorption case of atoms and bulk, the formation energy (E_f) was defined as

$$E_f = E_{Ag\ cluster/\ graphdiyne} - (E_{\ graphdiyne} + E_{Ag\ cluster})$$

where $E_{graphdiyne}$, $E_{Ag\ cluster}$ and $E_{Ag\ cluster/graphdiyne}$ are the total energy of the bulk graphdiyne, the energy of free Ag clusters in its bulk form, and the total energy of Ag clusters inserted in graphdiyne monolayer, respectively.

And for the adsorption configurations of small molecules (O_2 and H_2O), the adsorption energy (E_{ad}) was defined as

$$E_{ad} = E_{adsorbate/support} - (E_{adsorbate} + E_{support})$$

All three types of energies were derived from the scf calculations using the same calculated setting parameters. With this definition, a negative value indicates an exothermic adsorption and the more negative this value is, the more stable configuration has been proved.

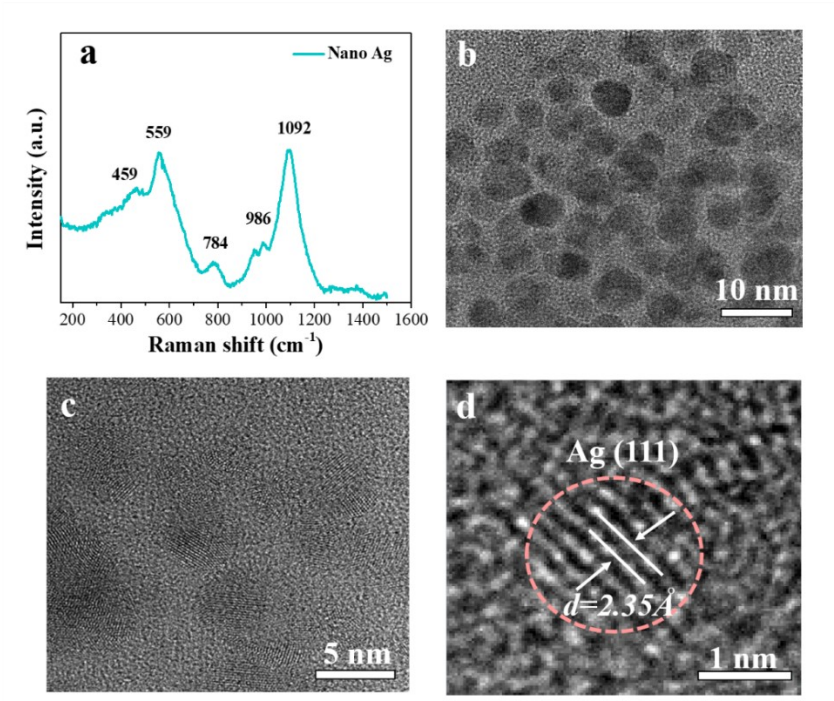

Figure S1. (a) The Raman spectrum of nano Ag. (b-d) HR-TEM images of nano Ag.

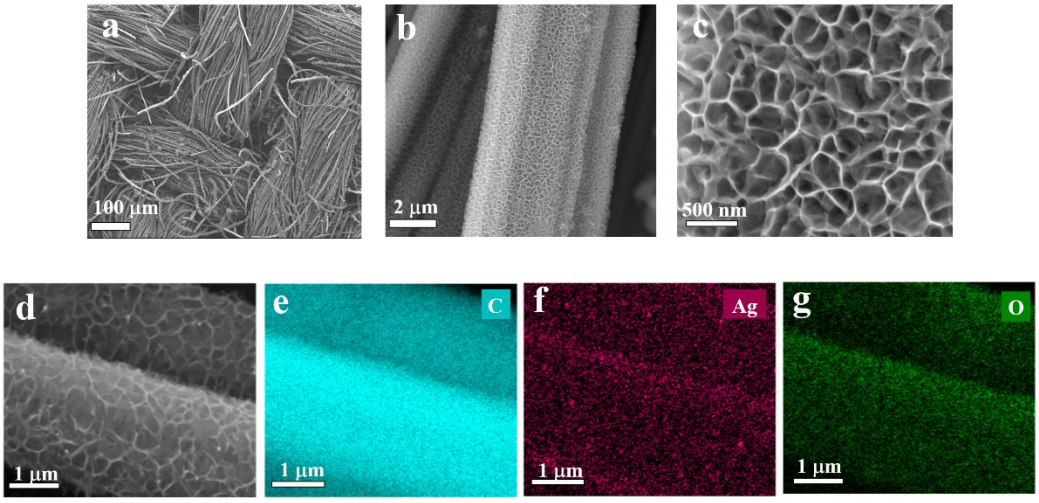

Figure S2. (a-c) SEM images of GDY with different magnifications. (d-g) SEM image and SEM-EDX mapping of Ag, C and O elements.

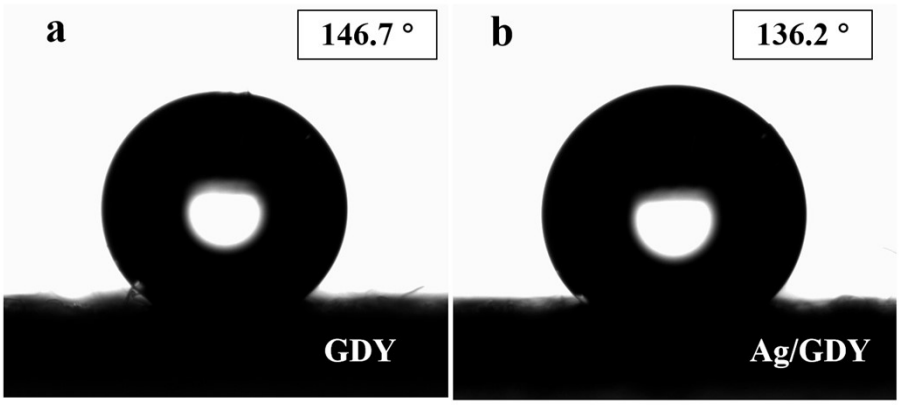

Figure S3. Contact angle measurements and wetting behavior of (a) bare GDY and (b) Ag/GDY.

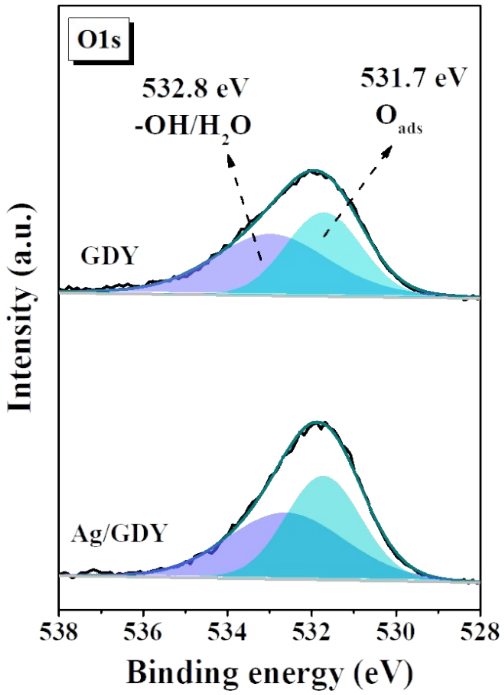

Figure S4. XPS O1s spectrum of Ag/GDY and GDY.

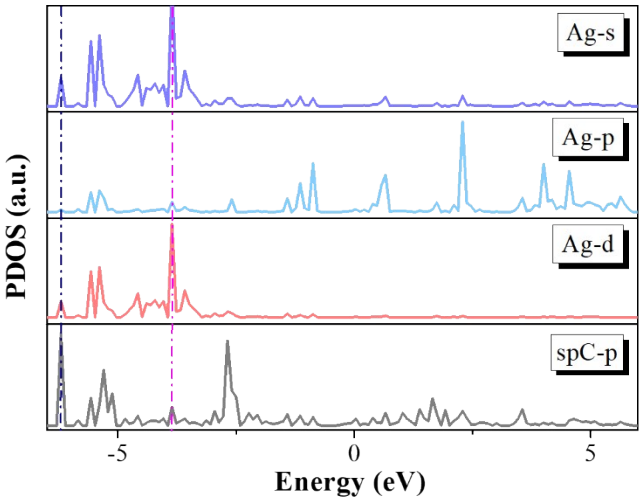

Figure S5. The corresponding spin-polarized partial density of states (PDOS) for the most stable nano Ag/GDY configuration. The vertical blue and pink dotted lines denote the hybridization between Ag atoms and sp C-p orbitals.

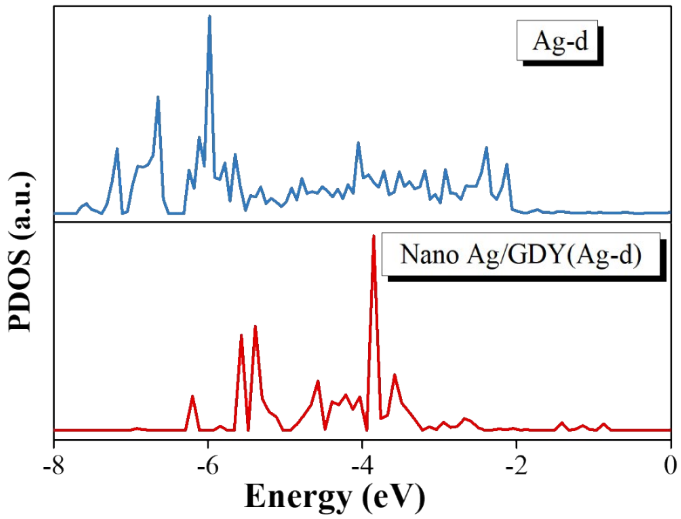

Figure S6. The partial density of states (PDOS) of the d bands for nano Ag and nano Ag on GDY. The Fermi level E_F was set to 0 eV.

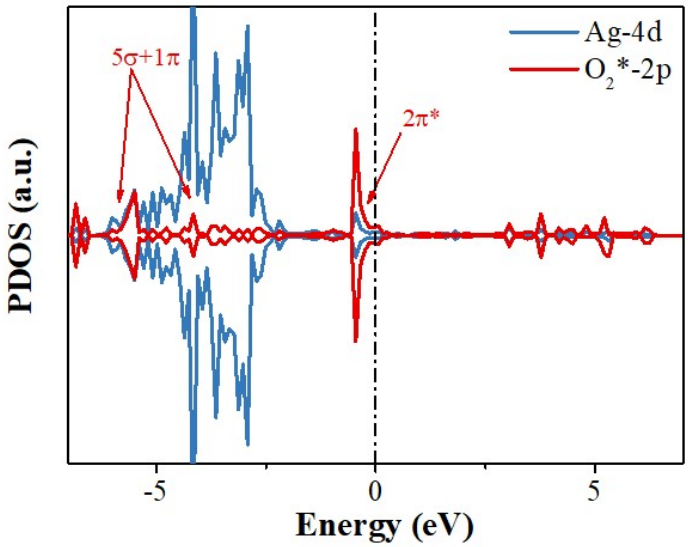

Figure S7. The corresponding spin-polarized partial density of states (PDOS) for the most stable O_2 adsorption on nano Ag/GDY. The vertical black dotted lines denote the Fermi level.

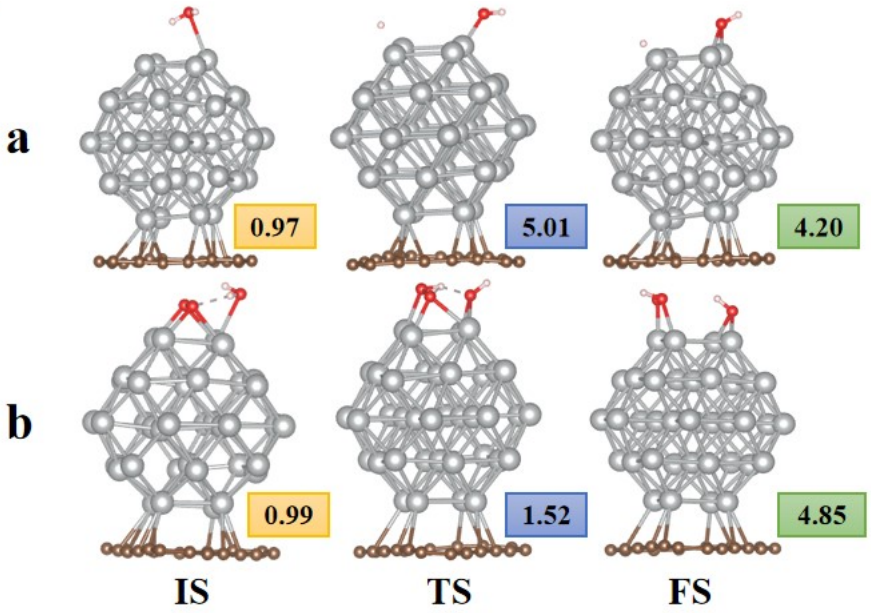

Figure S8. Optimized structures for the initial (IS, leftmost panels), transition (TS, central panels), and final (FS, rightmost panels) states of the most favorable path for the dissociation of: (a) H_2O, and (b) H_2O in the presence of co-adsorbed O_2 on nano Ag/GDY. The length of the cleaved O-H bond is given in angstroms (Å).

Table S1. The survival ratio of *E.coil* over Ag-based materials.

Materials	concentration	diameter	time	survival ratio	references
Ag/GDY	500 mg/L	2.5 nm	1 h	99%	This work
CuO/Ag	500 mg/L	≈35 nm	4 h	≈35%	[7]
ZnO/Ag	500 mg/L	≈35 nm	4 h	≈20%	[7]
CA/CNT/Ag	_	_	_	71%	[8]
GO/Ag	10 μL/mL	≈20 nm	1 h	≈60%	[9]
Ag/palygorskite	80 μg/mL	_	24 h	≈50%	[10]
Cotton/Ag/GQDs	_	8 nm	15 h	≈53%	[11]
Polyurethanes/Ag NPs	_	_	1 h	90.52%	[12]

Table S2. The fitting parameters of O1s results of GDY and Ag/GDY catalyst.

Sample	O species peak area	
	O_{ads}	H_2O/·OH
GDY	25049	28543
Ag/GDY	30826	31779

Table S3. The possible adsorption configurations (side-on and end-on) and adsorption energies of O_2 molecule on Ag_{38}/GDY at different sites (surface and interface sites)

Adsorption Site	Adsorption Configuration	Adsorption Energy (eV)	O-O band length (Å)
Surface Ag_{38}	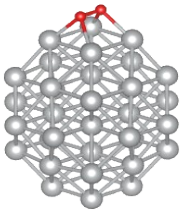	-1.60	1.24→1.45
Surface Site 1	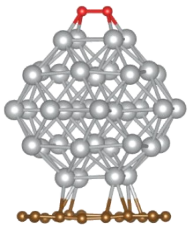	**-2.18**	**1.46**
Surface Site 2	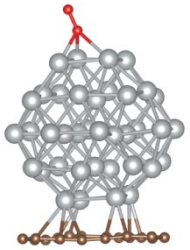	-1.57	1.32

Surface Site 3	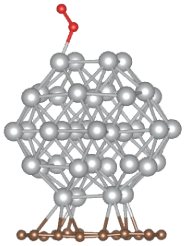	-1.39	1.31
Surface Site 4	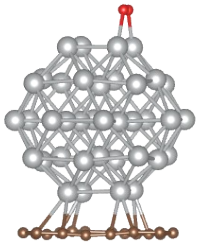	-1.31	1.36
Surface Site 5	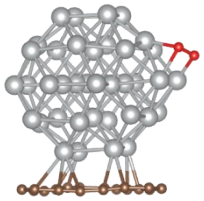	-1.53	1.42
Surface Site 6	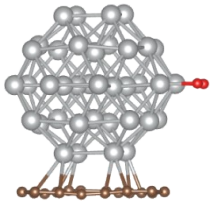	-1.52	1.36
Surface Site 7	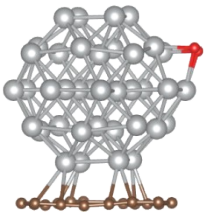	-1.52	1.44
Surface Site 8	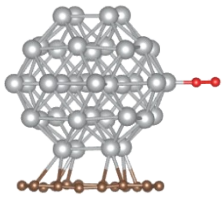	-1.15	1.24
Surface Site 9	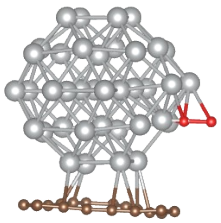	-1.30	1.36

Surface Site 10	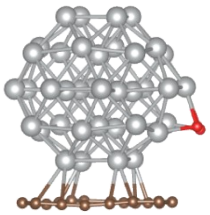	-1.71	1.42
Surface Site 11	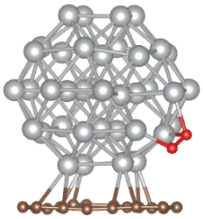	-1.74	1.42
Surface Site 12	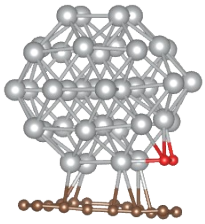	-1.34	1.45
Interface Site 1	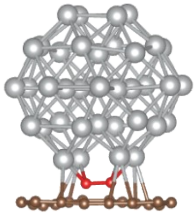	-1.60	1.40
Interface Site 2	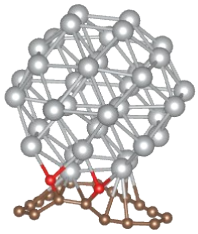	-3.19	2.60
Interface Site 3	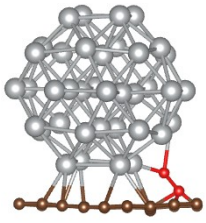	-0.74	1.43

Table S4. The possible adsorption configurations and adsorption energies of H_2O molecule on Ag_{38}/GDY at different sites (surface and interface sites) *Means water molecule will dissociate spontaneously after structure optimization.

Adsorption Site	Adsorption Configuration	Adsorption Energy (eV)	Ag-O band length (Å)
Surface Ag_{38}	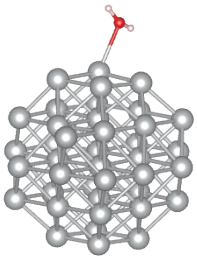	7.40	2.67
Surface Ag_{38}*	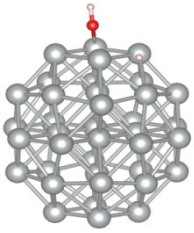	7.68	2.26
Surface Site 1	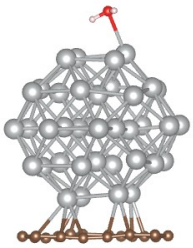	**-1.74**	**2.66**
Surface Site 2*	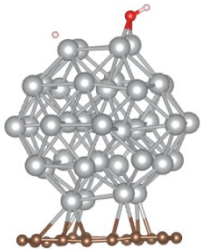	-1.37	2.20
Surface Site 3	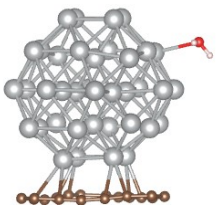	-1.70	2.64

Surface Site 4	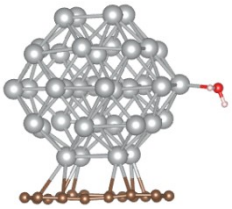	-1.70	2.59
Surface Site 5	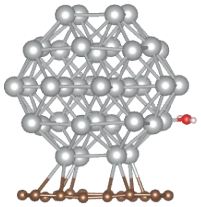	-1.67	2.65
Surface Site 6	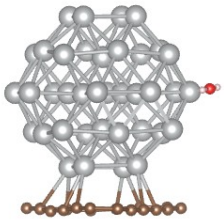	-1.70	2.65
Surface Site 7	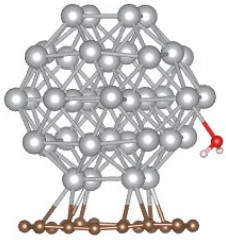	-1.70	2.56
Surface Site 8	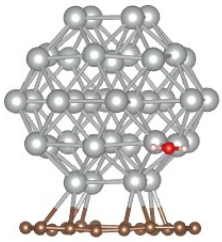	-1.70	2.58
Surface Site 9	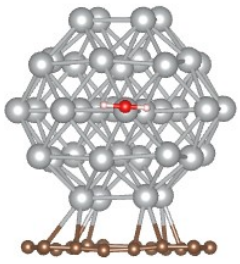	-1.69	2.61

Surface Site 10	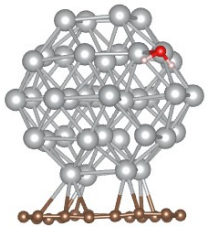	-1.69	2.62
Interface Site 1	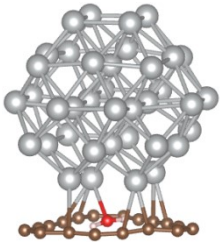	-1.50	2.56
Interface Site 2*	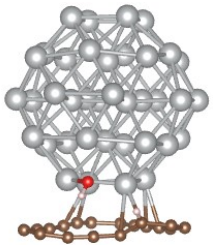	-0.88	2.15

Table S5. The possible co-adsorption configurations and co-adsorption energies of O_2 and H_2O molecule on Ag_{38}/GDY at different sites (surface and interface sites). O* means single oxygen atom from oxygen molecules on Ag_{38}/GDY.

Adsorption Site	Adsorption Configuration	Adsorption Energy (eV)	Nearest O*-H band length (Å)
Surface Co Site 1	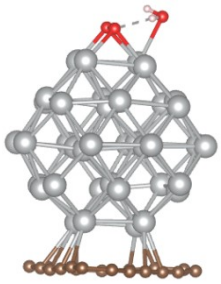	**-3.93**	**1.96**
Surface Co Site 2	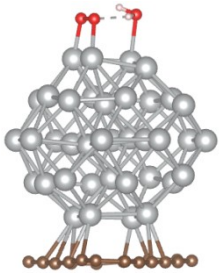	-3.78	1.86
Interface	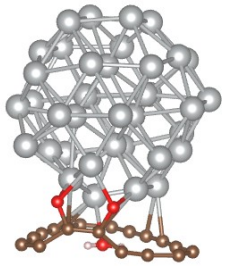	-0.96	3.59

References

[1] G. Kresse and J. Furthmüller, Efficiency of Ab-Initio Total Energy Calculations for Metals and Semiconductors Using a Plane-Wave Basis Set. *Comput. Mater. Sci.* 1996, **6**, 15-50.

[2] J. P. Perdew, K. Burke and M. Ernzerhof, Generalized Gradient Approximation Made Simple. *Phys. Rev. Lett.* 1996, **77,** 3865–3868.

[3] P. E. Blöchl, Projector Augmented-Wave Method. *Phys. Rev. B.* 1994, **50**, 17953–17979.

[4] G. Henkelman, B. P. Uberuaga and H. Jónsson, A Climbing Image Nudged Elastic Band Method for Finding Saddle Points and Minimum Energy Paths. *J. Chem. Phys.* 2000, **113**, 9901–9904.

[5] A. Heyden, A. T. Bell and F. J. Keil, Efficient Methods for Finding Transition States in Chemical Reactions: Comparison of Improved Dimer Method and Partitioned Rational Function Optimization Method. *J. Chem. Phys.* 2005, **123**, 224101.

[6] B. Hammer and J. K. Nørskov, Theoretical Surface Science and Catalysis—calculations and Concepts. *Adv. Catal.* 2000, **45**, 71–129..

[7] R. Asamoah, E. Annan, B. Mensah, P. Nbelayim, V. Apalangya, B. Onwona-Agyeman and A. Yaya, A Comparative Study of Antibacterial Activity of CuO/Ag and ZnO/Ag Nanocomposites. *Adv. Mater. Sci. Eng.* 2020, 1–18.

[8] A. W. Jatoi, H. Ogasawara, I. S. Kim and Q.-Q. Ni, Cellulose Acetate/Multi-Wall Carbon Nanotube/Ag Nanofiber Composite for Antibacterial Applications. *Mater. Sci. Eng. C.* 2020, **110**, 110679.

[9] L. Huang, H. Yang, Y. Zhang and W. Xiao, Study on Synthesis and Antibacterial Properties of Ag NPs/GO Nanocomposites. *J. Nanomater.* 2016, 1–9.

[10] Q. He, Q. Chen, R. Zhu, J. Du, S. He, G. Lv, C. Gu and A. Wang, Palygorskite Supporting Homogeneously Dispersed Ag Nanoparticles: Molten Salt Method and Enhanced Antibacterial Performance. *Clays Clay Miner.* 2023, 1–15.

[11] S. Luo, L. Fan, K. Yang, Z. Zhong, X. Wu and T. Ren, In Situ and Controllable Synthesis of Ag NPs in Tannic Acid-Based Hyperbranched Waterborne Polyurethanes to Prepare Antibacterial Polyurethanes/Ag NPs Composites. *RSC Adv.* 2018, **8**, 36571–36578.

[12] H. Teymourinia, O. Amiri and M. Salavati-Niasari, Synthesis and Characterization of Cotton-Silver-Graphene Quantum Dots (Cotton/Ag/GQDs) Nanocomposite as a New Antibacterial Nanopad. *Chemosphere* 2021, **267**, 129293.